JOURNAL OF GUIDANCE, CONTROL, AND DYNAMICS
Vol. 22, No. 2, March–April 1999

Electric Propulsion for Remote Sensing from Low Orbits

M. Guelman* and A. Kogan†
Technion—Israel Institute of Technology, 32000 Haifa, Israel

Low-altitude, low-eccentricity orbits allow high-resolution imagery of the Earth surface, but this advantage is usually neglected because of their poor coverage properties. Electric propulsion capability helps a remote sensing satellite to combine high resolution with short revisit times. Low-thrust control of the orbital period can make the spacecraft pass over prescribed areas on the terrestrial surface. The relevant optimal problem is finding a trajectory that passes over all given points during a given temporal interval. A corresponding thrust program is to minimize the fuel consumption. Its solution shows that the application of electric propulsion is quite practical. A small satellite with a modest initial-to-dry mass ratio and a feasible power supply may operate for years, decreasing the average revisiting time drastically in comparison with a noncontrolled orbit.

Nomenclature

a	= nongravitational acceleration of the spacecraft
C	= amplitude of radial thrust component
c	= exhaust jet velocity
c_{ij}	= spline coefficients
e	= eccentricity
h	= time increment
i	= equatorial inclination
l, m	= coordinates of a node of the grid associated with the site of interest
M	= mass of the satellite
$\boldsymbol{M}$	= matrix of the simultaneous set of linear equations
n	= mean motion of the satellite
P	= probability
p	= semilatus rectum
r	= geocentric distance
T	= orbital period
t	= current time
u	= $\omega + \nu$
W	= output power of the electrical propulsion system
x, y, z	= orbital coordinates
$\alpha, \beta, \gamma, \delta$	= special osculating elements
ζ	= attenuation decrement of the altitude oscillation
Θ	= annealing temperature
λ	= geographic longitude
μ	= Earth gravity parameter
ν	= true anomaly
σ	= standard deviation
τ	= special osculating element
Φ	= quality criterion
φ	= geographic latitude
ω	= argument of perigee

Introduction

ELECTRIC thrusters have specific impulses from 5 to 10 times that available from chemical thrusters, thus drastically reducing the propellant requirements for a given mission. The major operational uses of electric propulsion have been east–west station keeping and north–south station keeping.[1] These operations consist of attitude control and maneuvers required to maintain the desired orbit and phase against longitudinal harmonics of the terrestrial gravity field and local accelerations due to lunar and solar gravitational forces, as well as drag and solar pressure.

Received Feb. 11, 1998; revision received Sept. 30, 1998; accepted for publication Nov. 13, 1998.

*Professor, Faculty of Aerospace Engineering.
†Senior Scientist, Asher Space Research Institute.

During the last decade many new concepts were advanced on possible uses of electric propulsion for a variety of missions, such as orbit transfer,[2] formation flying,[3] interplanetary flight,[4] and many others.

Most optical remote sensing spacecraft were designed to orbit at altitudes where residual air drag is compatible with lifetimes of several years, thereby necessitating the use of large optical systems. An ion propulsion system, which has a high specific impulse, was proposed[5,6] for compensation of the air drag in an efficient way. This could result in routine operation at much lower altitudes, allowing the linear dimensions of the onboard instrumentation to be much smaller and the volume and mass of the spacecraft to be correspondingly lower. However, because the swath width is proportional to the orbit height,[7] low-altitude orbits may result in lack of coverage capability. This makes higher orbits, in spite of resolution loss, almost a necessity. Nevertheless, the use of electric propulsion can provide the means to control the orbit in such a way that coverage capability can still be achieved at low orbit altitudes. This is the main motivation of the work.

There are two different types of remote sensing operations, surveillance and reconnaissance. Surveillance is supervision over the entire Earth or an area with a size far exceeding the swath width. Duration of a surveillance cycle is inversely proportional to resolution and cannot be decreased by orbital maneuvering. Reconnaissance is observation of discrete sites of interest. With unlimited maneuvering capability, the trajectory may be designed so that the spacecraft will visit all given sites within an arbitrary time period. Electric propulsion gives large, but finite, maneuverability. The subject of this study is the evaluation of time period reduction through orbital maneuvering with electric propulsion.

The maneuvering strategy is control over the orbital period. It is intended to provide the spacecraft the ability to pass over the prescribed sites on the terrestrial surface at specific times. Given the site, a visiting time may be chosen only from a discrete set of opportunities that appear at the instants when the site on the rotating Earth crosses the orbital plane.

The trajectory in question is not unique. We specify the solution as the one supplying minimum fuel mass consumption.

The procedure of optimal orbit planning consists of two steps, piecewise optimization and scheduling. The first step is building a piecewise optimal trajectory that connects the pairs of sequential visiting points. Pontryagin's principle reduces the problem to a set of two-point boundary value problems for the ordinary differential equations. In our case it allows a general analytic solution.

Scheduling is global optimization of the trajectory by proper choice of passage times. Because the passage times may be selected only from a discrete set of opportunities, it is a discrete optimization problem. The simulated annealing method[8] provides an effective tool to solve it. Here its particular implementation is based on the

explicit formulas of piecewise optimization obtained at the first step. The minimization problem is reduced to a well-determined set of algebraic linear equations.

Once the schedule is compiled, the partial optimal arcs are integrated in a single trajectory. It is proved to be a specific kind of cubic spline.

In general, eccentricity perturbed by control thrust behaves like a random walk. To avoid its growth above an acceptable level, a small term suppressing the height oscillations is added to the thrust control program. Additional fuel consumption is negligibly small.

Problem Formulation

Consider a satellite in a circular orbit with period T and inclination i. Assume that it is subject only to the Newtonian attraction toward the Earth center. Let u denote its argument of latitude. If the current time t is initiated at the moment of passing the ascending node, then the geographic coordinates (φ, λ) of the subsatellite point satisfy the equations[9]

$$\sin\varphi = \sin i \sin u \tag{1a}$$

$$\tan\Lambda = \cos i \tan u \tag{1b}$$

$$\lambda = \Lambda - (2\pi/T_0)t \tag{1c}$$

$$\frac{\mathrm{d}\tilde{u}}{\mathrm{d}t} = \frac{2\pi}{T} \tag{1d}$$

where T_0 is a day, $u = v + \omega$, with v and ω the true anomaly and argument of perigee, respectively, and $\mathrm{d}\tilde{u}/\mathrm{d}t = (\mathrm{d}u/\mathrm{d}t) + eF(t)$ is mean motion, with e the orbit eccentricity and F a periodic function of time.

Given a list of sites on the terrestrial surface with geographic coordinates (φ_k, λ_k) to be covered, a corresponding list of (t_k, u_k) is

$$t_k = \left(\arctan\frac{\sin\varphi_k \cos i}{\sqrt{\sin^2 i - \sin^2\varphi_k}} - \lambda_k\right)\frac{T_0}{2\pi} \tag{2a}$$

$$u_k = \operatorname{acrsin}\frac{\sin\varphi_k}{\sin i} \tag{2b}$$

The (t_k, u_k) values are not unique because $t_k + lT_0$ may be chosen instead of t_k, as well as $u_k + 2m\pi$ instead of u_k with arbitrary positive integers l, m.

Electric propulsion allows one to control T so that the satellite can pass over all prescribed sites. Obviously, this can be done in many ways. We look for the trajectory with minimum fuel consumption.

Let c, a, M, and W be the exhaust jet velocity, the satellite acceleration, the satellite mass, and the output power of the propulsion unit. We assume the latter to be constant. Because $aM = \dot{M}c$ and $W = \dot{M}c^2$, it is easy to prove that $\dot{M} = (a^2M^2/W)$, and hence total fuel consumption is

$$\Delta M = \int_0^{t_f} \dot{M}\,\mathrm{d}t = \frac{1}{W}\int_0^{t_f} (aM)^2\,\mathrm{d}t \tag{3}$$

The problem formulation is, therefore, as follows. Given a set of points with geographic coordinates (φ_j, λ_j), $j = 1, \ldots, k$, the reconnaissance duration t_f, inclination i, and period T of the nominal orbit and available power W, select a set of integers (l_j, m_j), the thrust acceleration program $a(t)$, and the trajectory $u(t)$, such that the satellite passes over every given point and minimizes ΔM.

Piecewise Optimal Thrust Program

Let the spacecraft orbit have an eccentricity $e \ll 1$. Consider a Cartesian frame xyz that rotates uniformly with an angular rate $n_0 = \sqrt{(\mu/r_0^3)}$, where μ is the gravity parameter of the Earth. Let the center of the Earth lie at $(-r_0, 0, 0)$, the z axis be perpendicular to the spacecraft orbital plane, and the y axis be (almost) tangential to the spacecraft orbit. The equations of spacecraft motion referred to the frame thus defined are

$$\ddot{x} = 2n_0\dot{y} + n_0^2(x + r_0) - (\mu/R^3)(x + r_0) + a_x \tag{4a}$$

$$\ddot{y} = -2n_0\dot{x} + n_0^2 y - (\mu/R^3)y + a_y \tag{4b}$$

$$\ddot{z} = -(\mu/R^3)z + a_z \tag{4c}$$

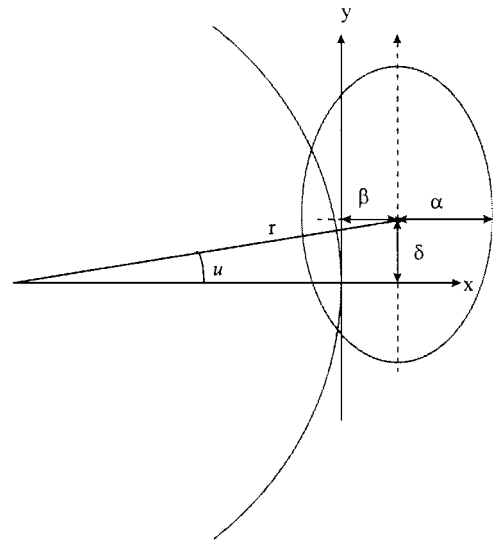

Fig. 1 Osculating parameters geometry.

where $R^2 = (x + r_0)^2 + y^2 + z^2$ and a_x, a_y, a_z are the components of the control acceleration.

Assuming $|x|$, $|y|$, and $|z|$ much smaller than r_0, linearization of Eq. (4) provides the well-known Hill equations[10]

$$\ddot{x} = 2n_0\dot{y} + 3n_0^2 x + a_x \tag{5a}$$

$$\ddot{y} = -2n_0\dot{x} + a_y \tag{5b}$$

$$\ddot{z} = -n_0 z + a_z \tag{5c}$$

For the force-free motion, i.e., $a_x = a_y = a_z = 0$, the general solution is given by

$$x(t) = \alpha\cos[n_0(t - \tau)] + \beta \tag{6a}$$

$$y(t) = -2\alpha\sin[n_0(t - \tau)] + \delta \tag{6b}$$

$$z(t) = \gamma\cos[n_0(t - \tau')] \tag{6c}$$

Parameters α, β, γ, τ, and τ' are arbitrary integration constants, whereas δ is a linear function of time, $\dot{\delta} = -\frac{3}{2}\beta$.

Figure 1 shows the geometric interpretation of the orbital parameters. A trajectory in the rotating frame is an elliptic epicycle that drifts slowly along the nominal circular orbit. The spacecraft runs along the epicycle in the clockwise direction with the period equal to the nominal one. The epicycle is an ellipse with the principal axes ratio equal to two. The actual orbit motion can be divided into secular (drift) and oscillatory (orbiting the epicycle) components.

The parameters α, β, γ, τ, and τ' can be expressed in terms of the spacecraft coordinates and velocities as follows:

$$\alpha = \sqrt{n_0^{-2}\dot{x}^2 + \left(3x + 2n_0^{-1}\dot{y}\right)^2} \tag{7a}$$

$$\beta = 4x + 2n_0^{-1}\dot{y} \tag{7b}$$

$$\gamma = \sqrt{z^2 + n_0^{-2}\dot{z}^2} \tag{7c}$$

$$\tau = -n_0^{-1}\arctan\frac{\left(3x + 2n_0^{-1}\dot{y}\right)\sin t - n_0^{-1}\dot{x}\cos t}{-\left(3x + 2n_0^{-1}\dot{y}\right)\cos t - n_0^{-1}\dot{x}\sin t} \tag{7d}$$

$$\tau' = -n_0^{-1}\arctan\frac{-z\sin t - n_0^{-1}\dot{z}\cos t}{z\cos t - n_0^{-1}\dot{z}\sin t} \tag{7e}$$

As already noted, the secular drift term of y is δ. Therefore, the secular behavior of y follows the equation

$$\dddot{y} = -3n_0^{-1}a_y \tag{8}$$

The actual value of y differs from $\tilde{y}$ by an oscillatory term proportional to e. We assume that the eccentricity is negligibly small and later show how to prevent its growth.

Equation (8) in polar coordinates (u, r) is

$$\frac{d^2u}{dt^2} = -\frac{3}{r}a_y \tag{9}$$

If $\Delta M \ll M$ and $a_r \equiv 0$, then

$$\Delta M = \frac{M^2}{W}\int_0^{t_f} a^2\,dt = \frac{(Mr)^2}{9W}\int_0^{t_f} (\ddot{u})^2\,dt \tag{10}$$

and minimum total fuel consumption is reached if

$$\Phi = \int_0^{t_f} (\ddot{u})^2\,dt \to \min \tag{11}$$

The optimal trajectory must minimize the criterion Φ and, simultaneously, meet the boundary conditions

$$\begin{aligned} u(t_k) &= u_k \qquad (k = 1, \ldots, k_f) \\ \dot{u}(t_0) &= \dot{u}_0, \qquad \dot{u}(t_f) = 0 \end{aligned} \tag{12}$$

It is well known from the classical calculus of variations[11] that the necessary condition for an extremum of a functional

$$\int_a^b F\left(x, y, y', y'', \ldots, y^{(n)}\right) dx$$

is Euler's equation

$$\frac{\partial F}{\partial y} - \frac{d}{dx}\frac{\partial F}{\partial y'} + \frac{d^2}{dx^2}\frac{\partial F}{\partial y''} - \cdots + (-1)^n \frac{d^n}{dx^n}\frac{\partial F}{\partial y^{(n)}} = 0 \tag{13}$$

In our case it reduces to

$$u^{(4)} = 0 \tag{14}$$

Its solution is a cubic spline connecting (t_k, u_k) ordered in time growth. Note that in contrast with classic cubic splines, this one has, generally speaking, a discontinuous second derivative. The discontinuity points are (t_k).

In the ith partial interval, the spline analytical expression is

$$u = c_{1i} + c_{2i}(t - t_i) + c_{3i}(t - t_i)^2 + c_{4i}(t - t_i)^3 \tag{15}$$

where

$$c_{1i} = u_i \tag{16a}$$

$$c_{2i} = \dot{u}_i \tag{16b}$$

$$c_{3i} = \frac{3(u_{i+1} - u_i) - (2\dot{u}_i + \dot{u}_{i+1})h_i}{h_i^2} \tag{16c}$$

$$c_{4i} = \frac{2(u_i - u_{i+1}) + (\dot{u}_i + \dot{u}_{i+1})h_i}{h_i^3} \tag{16d}$$

and $h_i = t_{i+1} - t_i$. The boundary conditions fix the values of u_i, whereas $u_i'(i > 1)$ are free parameters. At the scheduling stage, we use them to minimize Φ. An increment of Φ over the same partial interval is

$$\Delta_i \Phi = c_{3i}^2 h_i + 3c_{3i}c_{4i}h_i^2 + 3c_{4i}^2 h_i^3 \tag{17}$$

with $\Phi = \Sigma \Delta_i \Phi$. A comparison of Eqs. (17) and (16) shows that Φ is a quadratic function of du_i/dt. In this particular case, the necessary conditions for optimality are

$$\frac{\partial \Phi}{\partial \dot{u}_j} = \sum_i \left[(2c_{3i} + 3c_{4i}h_i)h_i \frac{\partial c_{3i}}{\partial \dot{u}_j} + (3c_{3i} + 6C_{4i}h_i)h_i^2 \frac{\partial c_{4i}}{\partial \dot{u}_j}\right] = 0 \tag{18}$$

Thereby, the minimization problem reduces to the solution of a set of linear algebraic equations with respect to $\dot{u}_i$. Because this set has a unique solution, it is the sufficient condition as well.

From Eqs. (16c), (16d), and (17), one can see that $\partial c_{3i}/\partial \dot{u}_j = \partial c_{4i}/\partial \dot{u}_j = 0$, except for $i = j$ and $i = j + 1$. Calculating $\partial \Phi/\partial \dot{u}_i$, it follows that

$$\frac{\partial \Phi}{\partial \dot{u}_1} = 2\left(\frac{\dot{u}_2}{h_1} + \frac{\dot{u}_1}{h_1}\right) - \frac{3}{h_1^2}(u_2 - u_1) = 0$$

$$\frac{\partial \Phi}{\partial \dot{u}_i} = 2\left(\frac{\dot{u}_{i+1}}{h_i} + \frac{h_i + h_{i-1}}{h_{i-1}h_i}\dot{u}_i + \frac{\dot{u}_{i-1}}{h_{i-1}}\right) - \frac{3}{h_i^2}(u_{i+1} - u_i)$$

$$- \frac{3}{h_{i-1}^2}(u_i - u_{i-1}) = 0 (1 < i < N) \tag{19}$$

$$\frac{\partial \Phi}{\partial \dot{u}_N} = 2\left(\frac{\dot{u}_N}{h_{N-1}} + \frac{\dot{u}_N}{h_N} + \frac{\dot{u}_{N-1}}{h_{N-1}}\right)$$

$$+ 3\left(\frac{u_N}{h_N^2} - \frac{u_N}{h_{N-1}^2} + \frac{u_{N-1}}{h_{N-1}^2}\right) = 0$$

This implies a set of linear equations $\boldsymbol{M}U = Z$, where $U = (\dot{u}_1, \ldots, \dot{u}_N)^T$,

$$Z = 3\begin{pmatrix} h_1^{-2} & 0 & 0 & \cdots & 0 & 0 \\ h_1^{-2} & h_2^{-2} & 0 & \cdots & 0 & 0 \\ 0 & h_2^{-2} & h_3^{-2} & \cdots & 0 & 0 \\ \cdots & \cdots & \cdots & \cdots & \cdots & \cdots \\ 0 & 0 & 0 & \cdots & h_{N-1}^{-2} & 0 \\ 0 & 0 & 0 & \cdots & h_{N-1}^{-2} & h_N^{-2} \end{pmatrix} \begin{pmatrix} u_2 - u_1 \\ u_3 - u_2 \\ u_4 - u_3 \\ \cdots \\ u_N - u_{N-1} \\ -u_N \end{pmatrix} \tag{20}$$

and

$$\boldsymbol{M} = 2 \cdot \begin{pmatrix} h_1^{-1} & h_1^{-1} & 0 & 0 & 0 & : & 0 & 0 \\ h_1^{-1} & h_1^{-1} + h_2^{-1} & h_2^{-1} & 0 & 0 & : & 0 & 0 \\ 0 & h_2^{-1} & h_2^{-1} + h_3^{-1} & h_3^{-1} & 0 & : & 0 & 0 \\ 0 & 0 & h_3^{-1} & h_3^{-1} + h_4^{-1} & h_4^{-1} & : & 0 & 0 \\ \cdots & \cdots & \cdots & \cdots & \cdots & \cdots & \cdots & \cdots \\ 0 & 0 & 0 & 0 & 0 & : & h_{N-2}^{-1} + h_{N-1}^{-1} & h_{N-1}^{-1} \\ 0 & 0 & 0 & 0 & 0 & : & h_{N-1}^{-1} & h_{N-1}^{-1} + h_N^{-1} \end{pmatrix} \tag{21}$$

$\boldsymbol{M}$ is tridiagonal, nonsingular, and in most cases (when the variation of h_i is not too large) well conditioned. Indeed, it permits the following decomposition:

$$\boldsymbol{M} = 2 \cdot \left(\begin{array}{ccc:ccc} h_1^{-1} & 0 & 0 & 0 & 0 & 0 \\ h_1^{-1} & h_2^{-1} & 0 & 0 & 0 & 0 \\ 0 & h_2^{-1} & h_3^{-1} & 0 & 0 & 0 \\ \hdashline 0 & 0 & 0 & h_{N-2}^{-1} & h_{N-1}^{-1} & 0 \\ 0 & 0 & 0 & 0 & h_{N-1}^{-1} & h_N^{-1} \end{array}\right) \times \left(\begin{array}{ccc:ccc} 1 & 1 & 0 & 0 & 0 & 0 \\ 0 & 1 & 1 & 0 & 0 & 0 \\ 0 & 0 & 1 & 0 & 0 & 0 \\ \hdashline 0 & 0 & 0 & 0 & 1 & 1 \\ 0 & 0 & 0 & 0 & 0 & 1 \end{array}\right) \tag{22}$$

Clearly its eigenvalues are just $1/h_i$, which proves the earlier statement. Note that independent variation of c_{3i} or c_{4i} instead of $\dot{u}_i$ leads to ill-conditioned equations and to prohibitive computational instability.

Scheduling

Once the piecewise optimization problem is solved and the corresponding value of Φ is obtained, we turn to scheduling.

As noted, every point (t_k, u_k) generates a rectangular grid, with every node corresponding to the same point on the terrestrial surface. By that, two sets of integers, $\{l_k\}$ and $\{m_k\}$, are to be chosen so as to minimize Φ. Figure 2 shows two rectangular grids in solid and dashed lines corresponding to two different sites. The oblique line depicts the nominal orbit. The nodes supplying the minimum value to Φ are marked. Their choice is a discrete minimization problem. The procedure for its solution is basically the simulated annealing method (SAM).[7] It starts with an arbitrary initial schedule and improves it step by step.

Initial Scheduling

To accelerate the computation, a special procedure for generating an initial schedule had been tailored. It does not apply directly to the values of Φ. Nevertheless it provides a much better schedule than a randomly generated one.

Initial scheduling is the selection of the nodes closest to the line $u(t) = nt$. A grid associated with a node (t^*, u^*) is a set $\{(t^* + 2l\pi, u^* + 2m\pi)\}$ with any integers l and m. The problem is finding l, $0 < l < t_f$, and m that minimize

$$\left| m - u'(0)l - \frac{u'(0)t^* - u^*}{2\pi} \right|$$

The algorithm we apply to finding optimal l_{opt} and m_{opt} works as follows.

1) Put $l = 1$, $\delta = 1000$, and $m_{\text{opt}} = l_{\text{opt}} = 0$.

2) Calculate

$$m = \left\| u'(0) + \frac{u'(0)t^* - u^*}{2\pi} \right\|$$

where $\|x\|$ is the integer closest to x.

3) Calculate

$$\delta' = \left| m - u'(0)l - \frac{u'(0)t^* - u^*}{2\pi} \right|$$

4) If $\delta' < \delta$, then put $l_{\text{opt}} = l$, $m_{\text{opt}} = m$, and $\delta = \delta'$.

5) Here $l = l + 1$. If $l < t_f$, go to step 2; otherwise the calculation is over.

Furthermore, to exclude the appearance of intervals with large derivatives, the selected nodes are to be far enough from each other. To comply with this additional condition, different values of l are chosen for nodes belonging to different grids. After a node from the ith grid has been selected, a corresponding value of $l = l_{\text{opt}}$ is marked. When processing the following grids, the marked values of l are skipped. Figure 2 shows the process: the day-long intervals containing the selected nodes are marked with a thick line in the bottom of the plot. A node belonging to another grid may be selected only from the subintervals not yet marked.

The described algorithm gives a reasonably good schedule, but generally speaking, it is not optimal. SAM is employed to achieve a global optimum or at least to improve the preliminary solution.

SAM[8]

SAM is an effective means for finding a global minimum (or a suitable local minimum not too much shallower than the global one) among many local minima. Its peculiarity is that it does not provide a monotonic decrease of a function subject to minimization. From time to time it jumps uphill, thus helping to avoid being trapped in a shallow local minimum.

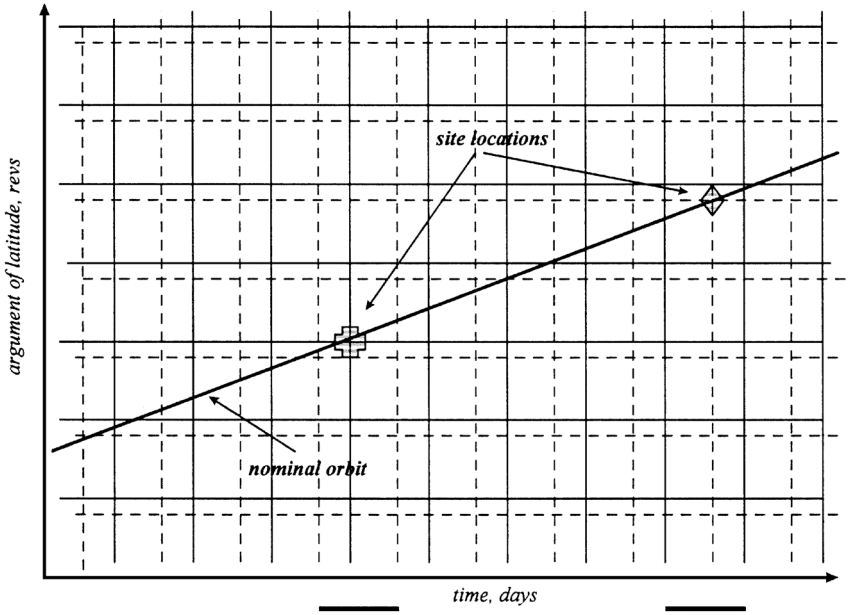

Fig. 2 Scheduling geometry.

The basic idea of SAM originates from thermodynamics of crystallization of liquids. A perfect crystal state corresponds to the global minimum of potential energy. Many other states, with different levels of regularity, also correspond to (local) minima. A well-known way to improve the crystal state of metals is annealing, i.e., heating up the sample and cooling it slowly. From time to time, the system spontaneously gets into a high-energy state, though the probability of such an event, in accordance with Bolzmann's law, decreases rapidly with decreasing temperature. This shakes the crystal grid and pushes the system away from a local potential pit, where it was before. The next temporary equilibrium state may be either in a deeper or in a shallower pit, but the probability of the former case prevails.

The SAM algorithm is essentially an organized random choice. It is randomized in two ways: 1) generating random 2-vector try steps and 2) accepting or rejecting a try step in accordance with a randomized procedure of decision making. Implementation of the latter is the key element of SAM. A dedicated part of the algorithm, the decision maker, approves every step downhill. If the step goes uphill, the decision maker draws lots (applies to a random generator). Actually, the procedure is more sophisticated than just tossing a coin. It takes into account 1) how high the step goes up and 2) how many successful steps have been done thus far. With j as the number of the current step, the SAM algorithm does the following.

1) It generates a random try step $(\delta l, \delta m)$ from the system current position (l_j, m_j) to a candidate position $(l_j + \delta l, m_j, +\delta m)$.

2) It calculates the quality functional $\Phi_{\text{new}} = \Phi(l_j + \delta l, m_j, +\delta m)$ in the alternate point.

3) It accepts the new state if $\Phi_{\text{new}} < \Phi = \Phi(l_j + \delta l, m_j + \delta m)$ and puts $\Phi = \Phi_{\text{new}}$, where $l_{j+1} = l_j + \delta l$, and $m_{j+1} = m_j + \delta m$.

4) Otherwise, a) it calculates the Bolzmann probability $P = \exp[(\Phi - \Phi_{\text{new}})/\Theta(j)]$; b) it draws lots, i.e., generates a random number ξ uniformly distributed within the interval (0, 1); c) if $\xi < P$, then it accepts the candidate step by putting $\Phi = \Phi_{\text{new}}$, where $l_{j+1} = l_j + \delta l$, and $m_{j+1} = m_j + \delta m$; d) otherwise it declines the candidate step, i.e., stays in the previous position.

5) If less than a predefined number N_{bad} of preceding try steps in succession go uphill, then the algorithm returns to point 1; otherwise it stops.

To run a SAM program, one needs an annealing plan, i.e., a law that governs the decrease of temperature $\Theta = \Theta(j)$. Its choice is a trade between speed and accuracy. We used a plan starting at $\Theta = 3\Phi_{\text{init}}$ and decreasing by a factor of 0.3 after each 25 attempts.

Scheduling provides us with the values of t_k and u_k. By substituting them into Eqs. (20) and (22) and solving equation $\boldsymbol{M}U = Z$, one obtains $U = (\dot{u}_1, \ldots, \dot{u}_N)^T$. Introducing U into Eq. (16), a complete set of spline coefficients c_{ij} is obtained. The trajectory is now given by Eq. (15).

Numerical Results

A small spacecraft with a total mass of 100 kg and input power of 200 W was considered for simulation. Figures 3–6 show an example of a trajectory. An initial set of points is marked in Fig. 3 with filled circles. A set of nodes provided by the optimization procedure is grouped close to the initial orbit.

It is important that deviation of the orbital mean motion from its nominal value is small, for it is roughly proportional to the flight altitude deviation. This may be critical at very low orbits because of the danger of atmospheric drag. Deviations shown in Fig. 4 correspond to altitude variation of less than 20 km.

The control acceleration program shown in Fig. 5 never exceeds 1 mm/s^2, which is well within the capability of small satellites driven by Hall thrusters.[12] The typical duration of a linear thrust program segment is a few days.

Total mass of consumed fuel is shown in Fig. 6. On average it is 5 g per day. A modest initial $m_{\text{fuel}}/m_{\text{total}}$ ratio of $\frac{1}{20}$ is sufficient to maintain controllable motion over 3 years.

The plots shown in Figs. 3–6 are quite typical. Other sets of randomly generated visiting sites give very similar trajectories and fuel consumption estimates, provided the total reconnaissance time duration and number of visiting sites are fixed (in the preceding example they are 50 days and 20 sites).

To obtain qualitative information on overall system performance a Monte Carlo simulation was carried out for a large number of cases as a function of total reconnaissance time and number of sites for sets of randomly generated visiting sites. Average fuel consumption rate vs total reconnaissance time and number of sites was determined for each case.

Based on the numerical results, a best-fit approximation to the average relative fuel consumption decimal logarithm vs reconnaissance time and number of sites was determined, using as reference the 50 days, 20 sites case. In Fig. 7, lines of constant decimal logarithm of average relative fuel consumption of the best-fit function are plotted. As can be seen, an increase or decrease of either reconnaissance time or number of sites affects fuel consumption in very different ways. For instance, duplication of the number of sites (from 20 to 40) increases the fuel mass consumption by approximately a factor of 60, whereas duplication of the reconnaissance time (from 50 to 100 days) decreases fuel consumption by approximately a factor of 300, that is, five times more.

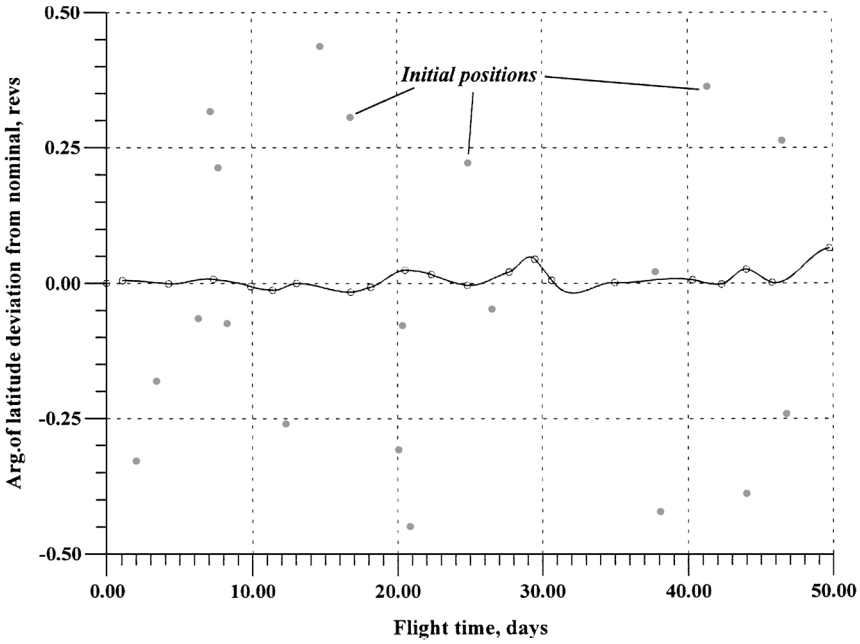

Fig. 3 Trajectory covering a given set of points; their initial positions are marked with solid circles.

Two remarks are in order.

1) The given estimates are valid under the assumption of random location of the requested sites. Otherwise, they are distorted. For instance, if monitoring of a single compact area is required, then daily revisiting is possible, practically without fuel consumption.

2) The right choice of the nominal orbital period is beyond the scope of this paper. Still it should be noted that its role is quite sensible.[13] Fuel savings by a factor of two or more can be achieved as compared with those plotted in Fig. 7.

Damping of Eccentricity Walk

When the itinerary includes many intermediate visiting points, the eccentricity behaves as a random walk. It may grow significantly and by that make the cubic spline approximation invalid. In the case of very low orbits (below some 200 km), growth of eccentricity is undesirable by itself, for it increases the atmospheric drag. To avoid these effects, a small term suppressing the altitude oscillations induced by eccentricity should be added to the thrust control.

Consider Eqs. (7) again. Equations that describe the effect of control thrust on the parameters $\alpha, \ldots, \tau'$, have the following structure:

$$\frac{\mathrm{d}q}{\mathrm{d}t} = \frac{\partial q}{\partial \dot{x}} a_x + \frac{\partial q}{\partial \dot{y}} a_y + \frac{\partial q}{\partial \dot{z}} a_z \qquad (q = \alpha, \ldots, \tau') \tag{23}$$

A straightforward calculation results in the following differential equation for the first of the parameters α:

$$\dot{\alpha} = \alpha^{-1}\left[n_0^{-2}\dot{x}a_x + 2n_0^{-1}\left(3x + 2n_0^{-1}\dot{y}\right)a_y\right] \tag{24}$$

By virtue of Eq. (4), an equivalent form of this equation is

$$\dot{\alpha} = -n_0^{-1}\left\{\sin[n_0(t-\tau)]a_x + \cos[n_0(t-\tau)]a_y\right\} \tag{25}$$

As shown earlier, an asymptotic solution of the optimal control problem is piecewise linear:

$$a_x \equiv 0, \qquad (a_y)_i = A_i + B_i(t - t_i) \tag{26}$$

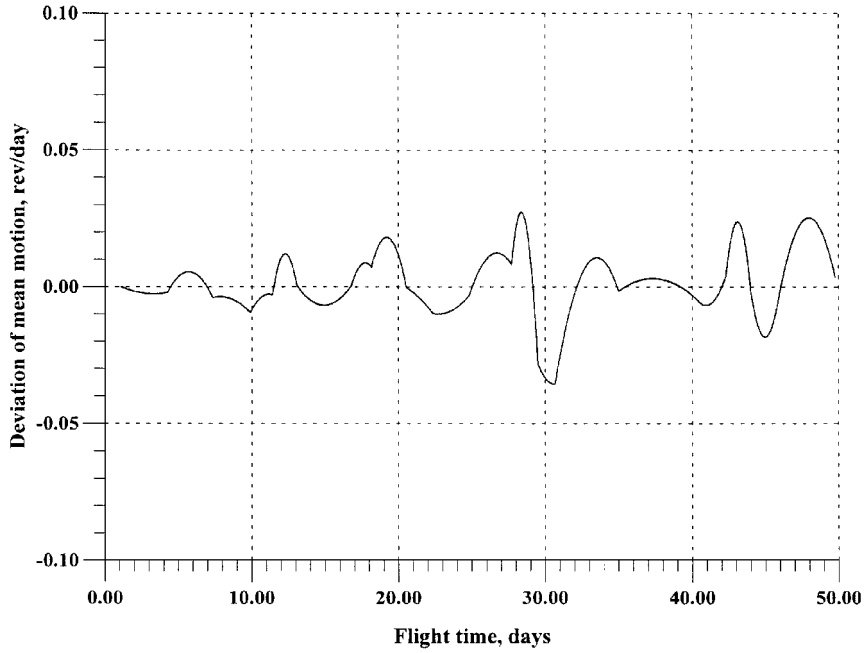

Fig. 4 Deviation of mean orbital motion from its initial value.

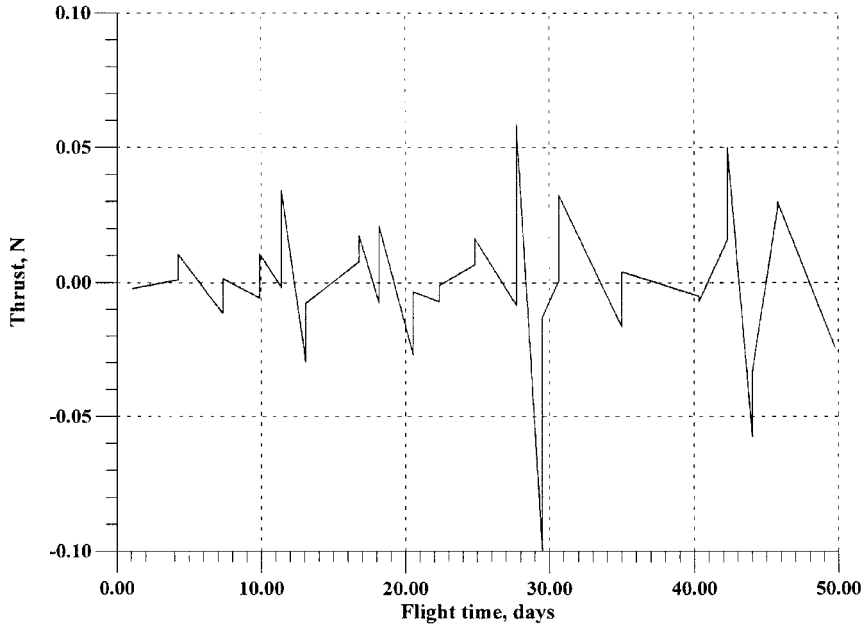

Fig. 5 Optimal thrust program; thrust vector is directed along (positive) or opposite (negative) the orbital velocity.

The nodes t_i are randomly distributed over the t axis. The slopes of the polygonal line (26) are also random (see Fig. 5). This control excites a random walk of eccentricity with amplitude α. A rigorous analysis of its statistical properties is beyond the scope of this work. Still a simple schematic consideration that follows will help to work out a control to suppress the random walk and to estimate roughly its damping efficiency.

Let $t_k < t < t_{k+1}$. Then integration of Eqs. (25) and (26) gives

$$\alpha(t) = \alpha(t_k) + n_0^{-3} B_k - n_0^{-2}[A_k + B_k \cdot (t - t_k)] \times \sin[n_0(t - t_k)] - n_0^{-3} B_k \cdot \cos[n_0(t - t_k)] \quad (27)$$

An increment $\delta\alpha_k = \alpha(t_{k+1}) - \alpha(t_k)$ is obviously independent of $\alpha(t_k)$. A natural assumption is that $\{B_k\}$ and $\{h_k\}$, $h_k = t_{k+1} - t_k$, are random sequences in which all terms are mutually independent and have the same distribution. In addition, the former sequence has a zero mean, otherwise the orbit would spiral systematically upward or downward. Under these assumptions, the increments $\delta\alpha_k$ are also centered, independent, and identically distributed. Moreover, in our case $n_0 h_k \gg 1$, and the same is true for its standard deviation. Thereby the variation of $\delta\alpha_k$ allows an estimate

$$\sigma^2 = \langle(\delta\alpha)^2\rangle = \tfrac{3}{2} n_0^{-6} \langle B^2\rangle + \tfrac{1}{2} n_0^{-4} (\langle A^2\rangle + \langle B^2\rangle \cdot \langle h^2\rangle) \quad (28)$$

where $\langle\rangle$ denotes mathematical expectation. Because

$$\alpha(t_k) = \alpha(t_0) + \sum_{i=0}^{k} \delta\alpha_k \quad (29)$$

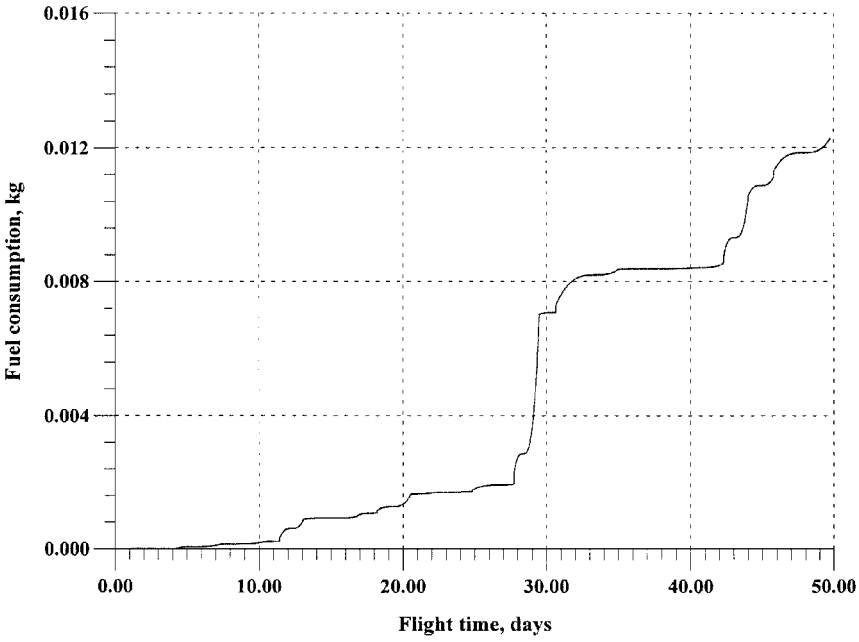

Fig. 6 Fuel consumption history.

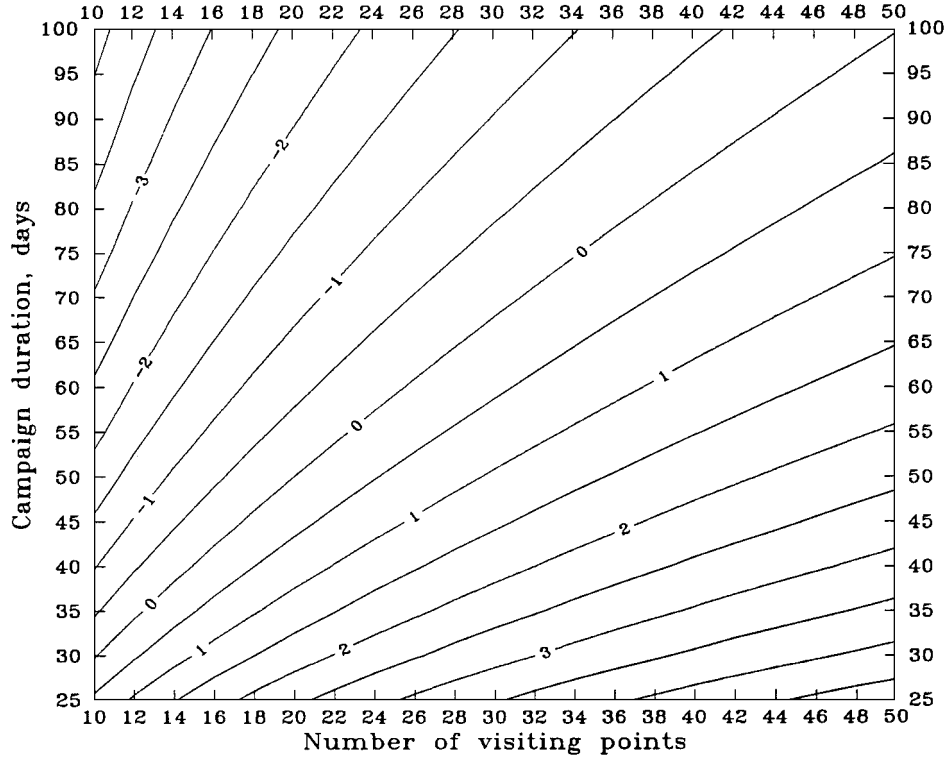

Fig. 7 Decimal logarithm of relative fuel consumption rate (best-fit approximation to the Monte Carlo generated data).

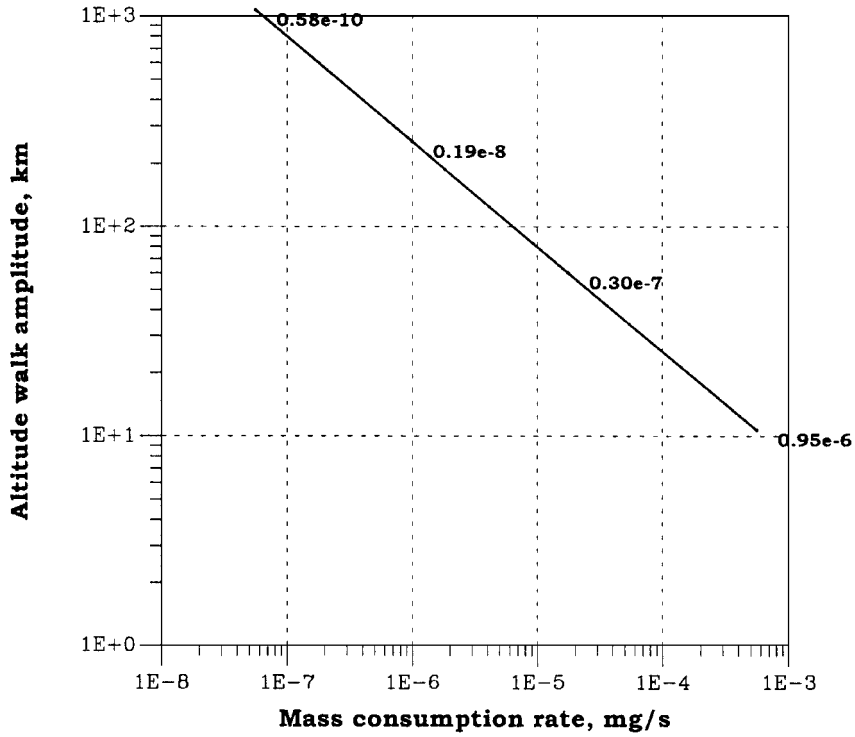

Fig. 8 Altitude walk amplitude and mass consumption rate, with C as parameter.

its variance is a sum of variances of $\delta\alpha_k$, which grows in rough proportion with k,

$$\text{var}[\alpha(t_k)] \approx k\sigma^2 \underset{k\to\infty}{\longrightarrow} \infty \tag{30}$$

Now add a_x to the control thrust as follows:

$$a_x = C\alpha \sin[n_0(t-\tau)] \tag{31}$$

where C is a positive constant. By virtue of Eq. (24) it provides an averaged equation

$$\alpha(t_{k+1}) = \zeta_k \alpha(t_k) + \delta\alpha_k \tag{32}$$

where

$$\zeta_k = \exp[-C(h_k/2n_0)] \tag{33}$$

and $\delta\alpha_k$ is the same random sequence as earlier. Inversion of the recursive formula (32) leads to

$$\alpha(t_k) = \zeta_{k-1}[\zeta_{k-2}(\cdots\{\zeta_1[\zeta_0\alpha(t_0) + \delta\alpha_0] + \delta\alpha_1\}\cdots) + \delta\alpha_{k-2}] + \delta\alpha_{k-1} \tag{34}$$

If $\langle\zeta_k\rangle \equiv \zeta < 1$, the variance of $\alpha(t_k)$ is

$$\text{var}[\alpha(t_k)] = \sigma^2(1 + \zeta^2 + \zeta^4 + \cdots + \zeta^{2k}) \underset{k\to\infty}{\longrightarrow} \sigma^2/1 - \zeta^2 \tag{35}$$

In contrast with Eq. (30), the variance tends to a finite limit. According to Eq. (33),

$$(1-\zeta^2)^{-1} = \{1 - \exp[-C(h/n_0)]\}^{-1} \approx [1 - 1 + (Ch/n_0)]^{-1} = n_0/Ch \tag{36}$$

By that the limiting value in Eq. (35) is

$$\text{var}(\alpha_\infty) = \sigma^2 n_0/Ch \tag{37}$$

The corresponding fuel consumption rate is, according to Eqs. (1) and (37),

$$\dot{M} = -\frac{(MC)^2}{W}\text{var}(\alpha) = -\frac{M^2C\sigma^2 n_0}{Wh} \tag{38}$$

Figure 8 shows the residual amplitude of altitude oscillation and fuel consumption rate vs C computed according to Eqs. (37) and (38).

The amplitude of random deviations along the nominal orbit is two times the deviation in altitude. To suppress the oscillations to an acceptable level, and with the spacecraft mass and power parameters taken above, fuel consumption of some 10 μg/s is required. This adds a few percent to the total fuel mass budget.

Conclusions

The orbit control of an electrically propelled remote sensing satellite was considered. Given a set of requested sites on the Earth surface, a reconnaissance campaign duration, and a satellite nominal orbit, a thrust acceleration program was obtained such that the trajectory will pass over all of the sites in the given reconnaissance time and such that the fuel requirement is a minimum. The optimal orbit was obtained through two sequential steps, phasing and scheduling. In phasing, a piecewise optimal trajectory was built to connect the arbitrarily picked pairs of visiting points. In scheduling, passing times over the requested sites are determined. This is shown to be a discrete optimization problem and is solved with the SAM. A globally optimal trajectory is proved to be a specific kind of cubic spline. Its calculation completes the solution. The fuel minimization problem is thus reduced to a set of algebraic linear equations coupling the spline coefficients. Finally, a thrust control term suppressing the orbit height oscillations was derived and added to the thrust control program to prevent an unacceptable eccentricity growth provoked by the main term of the thrust program.

Numerical simulations for the case of a small spacecraft were performed. The results clearly show that a small electrically propelled spacecraft can achieve both high resolution (low altitude) and low-average revisiting times.

References

[1] Pollard, J. E., Jackson, D. E., Marvin, D. C., Jenkin, A. B., and Janson, S. W., "Electric Propulsion Flight Experience and Technology Readiness," AIAA Paper 93-221, June 1993.

[2] Guelman, M., and Psiaki, M. L., "Electric Propulsion for Orbit Transfer in a Resistive Medium," *Journal of the Astronautical Sciences*, Vol. 44, No. 1, 1966, pp. 79–97.

[3] Janson, S. W., "The On-Orbit Role of Electric Propulsion," AIAA Paper 93-2220, June 1993.

[4]Meserole, J. S., and Richards, W. R., "Direct Trajectory Options Using Solar Electric Propulsion for the Pluto Fast Flyby," AIAA Paper 94-3253, June 1994.

[5]Reale, J., "A Low Altitude Ion Propelled Remote Sensing Spacecraft," Associazione Italiana de Aeronautica e Astronautica/AIAA/Deutsche Gesellschaft fuer Luft- und Raumfahrt/Japan Society for Aeronautical and Space Sciences 22nd International Electric Propulsion Conf., Viareggio, Italy, IEPC Paper 91-132, Oct. 1991.

[6]Fearn, D. G., "High Resolution Optimal Remote Sensing from a 200 kg-Class Spacecraft," 45th Congress of the International Astronautical Federation, Jerusalem, Israel, IAF Paper 94-B.2.072, Oct. 1994.

[7]Elachi, C., *Introduction to the Physics and Techniques of Remote Sensing*, Wiley, New York, 1987, pp. 393–404.

[8]Press, W. H., Teukolsky, S. A., Wetterling, W. T., and Flannery, B. T., *Numerical Recipes in Fortran. The Art of Scientific Computation*, 2nd ed., Cambridge Univ. Press, Cambridge, England, UK, 1992, pp. 107–110, 436–448.

[9]Battin, R. H., *An Introduction to the Mathematics and Methods of Astrodynamics*, AIAA Education Series, AIAA, New York, 1987, pp. 123–125.

[10]Kaplan, M. H., *Modern Spacecraft Dynamics and Control*, Wiley, New York, 1976, pp. 111–113.

[11]Sokolnikoff, I. S., *Mathematics of Physics and Modern Engineering*, 2nd ed., McGraw–Hill, New York, 1966, pp. 352, 353.

[12]Raitses, Y., Ashkenazy, J., and Guelman, M., "Propellant Utilization in Hall Thrusters," *Journal of Propulsion and Power*, Vol. 14, No. 2, 1998, pp. 247–254.

[13]Kogan, A., "Orbital Period Optimization for Remote Sensing Satellites," *Proceedings of the 38th Israel Annual Conference on Aerospace Sciences* (Tel Aviv, Israel), OMANUTH Press, Haifa, Israel, 1998, pp. 338–343.